

# Out of Length Text Recognition with Sub-String Matching

Yongkun Du<sup>1</sup>, Zhineng Chen<sup>1\*</sup>, Caiyan Jia<sup>2</sup> Xieping Gao<sup>3</sup> Yu-Gang Jiang<sup>1</sup>

<sup>1</sup>School of Computer Science, Fudan University, China

<sup>2</sup>School of Computer and Information Technology, Beijing Jiaotong University, China

<sup>3</sup>College of Information Science and Engineering, Hunan Normal University, China

ykdu23@m.fudan.edu.cn, {zhinchen, ygj}@fudan.edu.cn, cyjia@bjtu.edu.cn, xpgao@hunnu.edu.cn

## Abstract

Scene Text Recognition (STR) methods have demonstrated robust performance in word-level text recognition. However, in applications the text image is sometimes long due to detected with multiple horizontal words. It triggers the requirement to build long text recognition models from readily available short word-level text datasets, which has been less studied previously. In this paper, we term this the Out of Length (OOL) text recognition. We establish a new Long Text Benchmark (LTB) to facilitate the assessment of different methods in long text recognition. Meanwhile, we propose a novel method called OOL Text Recognition with sub-String Matching (SMTR). SMTR comprises two cross-attention-based modules: one encodes a sub-string containing multiple characters into next and previous queries, and the other employs the queries to attend to the image features, matching the sub-string and simultaneously recognizing its next and previous character. SMTR can recognize text of arbitrary length by iterating the process above. To avoid being trapped in recognizing highly similar sub-strings, we introduce a regularization training to compel SMTR to effectively discover subtle differences between similar sub-strings for precise matching. In addition, we propose an inference augmentation to alleviate confusion caused by identical sub-strings and improve the overall recognition efficiency. Extensive experimental results reveal that SMTR, even when trained exclusively on short text, outperforms existing methods in public short text benchmarks and exhibits a clear advantage on LTB. Code: <https://github.com/Topdu/OpenOCR>.

## 1 Introduction

Extracting text from natural images is a crucial and well-established task, typically encompassing scene text detection and recognition. In scene text recognition (STR), past research has achieved significant progress in word-level text recognition. However, in real-world applications, the text is not always detected as an individual word, but a line-level text sometimes. That is, text instances detected by scene text detectors may contain multiple horizontal words, presenting a long text recognition challenge. It is worth noting that existing STR datasets are predominantly compromised of word-level text, where long text like the aforementioned is scarce. Therefore, accurately recognizing long text by utilizing solely short word-level datasets has emerged as

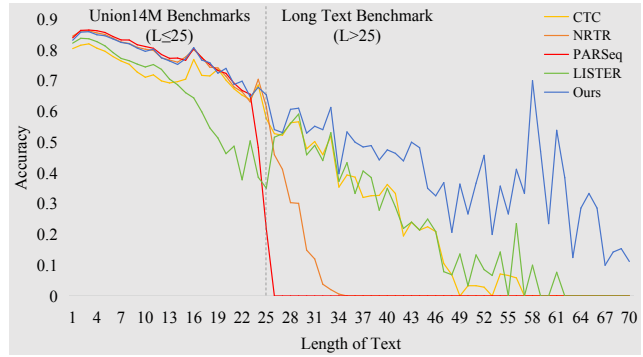


Figure 1: Attention-based methods like NRTR (Sheng, Chen, and Xu 2019) and PARSeq (Bautista and Atienza 2022) perform well in short text recognition, while the CTC-based FocalSVTR (CTC) and the length-insensitive LISTER (Cheng et al. 2023) outperform them in long text but worse in short text. Our proposed SMTR gets superior performance in both short and long text recognition.

a promising yet challenging frontier in STR, which we term Out of Length (OOL) text recognition in this paper.

Existing STR models are mostly designed towards recognizing short word-level text with no more than 25 characters, i.e.,  $L \leq 25$ . We establish the first Long Text Benchmark (LTB) that focuses on the long text ( $L > 25$ ), which will be detailed later. As shown in Fig. 1, we evaluate several popular STR models (Sheng, Chen, and Xu 2019; Bautista and Atienza 2022; Cheng et al. 2023) on LTB. The results show that the CTC-based method (Du et al. 2022) and LISTER (Cheng et al. 2023) can recognize long text due to their length extrapolation capabilities. However, their accuracy declines rapidly as text length increases. Additionally, these methods show a noticeable performance gap in short text recognition compared to the competitors (Sheng, Chen, and Xu 2019; Bautista and Atienza 2022), due to not being equipped with an advanced decoder. On the other hand, NRTR (Sheng, Chen, and Xu 2019) and PARSeq (Bautista and Atienza 2022), as representatives of the attention-based methods, typically employ the self-attention mechanism (Vaswani et al. 2017) to encode the decoded characters along with absolute positional information (Vaswani et al. 2017)

\*Corresponding Author

as the linguistic context or position-involved representation to aid decoders in accurately recognizing characters. This powerful approach enables these methods to achieve state-of-the-art results in short text recognition. However, they are unable to effectively learn the representation beyond the length of training text, which limits them from processing long text when trained solely on short text. Similar limitations are also observed in other attention-based methods (Shi et al. 2019; Li et al. 2019; Wang et al. 2021; Fang et al. 2021; Du et al. 2023; Zhang et al. 2023; Zheng et al. 2024).

In this paper, we introduce a novel method termed OOL text recognition with sub-string matching (SMTR), which achieves OOL text recognition by innovatively leveraging string-matching techniques. Specifically, SMTR recognizes text by first matching specified a sub-string within an image, and then positioning and recognizing the Next and Previous characters of the sub-string. SMTR gets rid of the linguistic context and the absolute position, recognizing text fully relying on sub-string patterns. This new paradigm is reasonable as both short and long text can be decomposed into multiple sub-string units. The matching process only compares a portion of text in the image with the sub-string, regardless of whether the text is short or long. Based on this fact, SMTR learns to match sub-strings by using only short text images but can still recognize long text.

To implement this, SMTR develops a lightweight architecture with a sub-string encoder and a sub-string matcher. The former encodes a sub-string as two representations referred to as next and previous queries. While the latter directs the two queries to attended visual features, aiming to accurately match the sub-string and recognize the next and previous characters. Within this new recognition paradigm, similar or repeated sub-strings in one text image inevitably hinder precise sub-string matching. To effectively screen for similar sub-strings, we propose a regularization training strategy that encourages SMTR to pay attention to the subtle differences between sub-strings, thus better distinguishing them. In addition, we introduce an inference augmentation strategy which breaks a long text image into different sub-images for independent processing, thus significantly alleviating the side affection caused by repeated sub-strings. Moreover, by processing these sub-images in parallel, SMTR improves the overall recognition efficiency remarkably. Experimental results demonstrate that SMTR achieves highly competitive performance on challenging short text benchmarks and exhibits a noteworthy advantage on LTB. The contributions are summarised as follows:

- We observe the requirement of building long text recognition models based on short text datasets. For the first time, we term this OOL text recognition challenge and establish a long text benchmark called LTB to assess the long text recognition capability of STR models.
- We propose SMTR, a novel method that innovatively incorporates string-matching techniques to address the OOL challenge. Meanwhile, regularization training and inference augmentation strategies are proposed to ensure precise recognition following this pipeline.
- SMTR achieves state-of-the-art performance on both

public short text benchmark and LTB, utilizing merely short text for training. This enriches the STR schemes in handling diverse applications.

## 2 Related Work

Existing STR methods mainly focus on word-level text recognition. Among them, attention-based (Lee and Osindero 2016) methods are intensively studied for their impressive performance. Some of these methods (Bautista and Atienza 2022; Yue et al. 2020; Wang et al. 2021; Du et al. 2023) use learnable position embeddings to accurately learn context information. However, because learnable position embeddings are typically not scalable, these methods can only recognize short text. In contrast, methods (Shi et al. 2019; Li et al. 2019; Sheng, Chen, and Xu 2019; Fang et al. 2021; Zhang et al. 2023; Zheng et al. 2024; Du et al. 2024) employ LSTM (Hochreiter and Schmidhuber 1997; Chung et al. 2014) or masked self-attention mechanism with sinusoidal positional encoding (Lee and Osindero 2016) to model context. They have some length extrapolation capability. Nevertheless, these models are primarily trained on short text. Therefore their inference ability is limited when dealing with long text, resulting in a significant decrease in recognition accuracy. Additionally, some methods do not rely on well-designed attention-based decoders, such as CTC-based (Graves et al. 2006) methods (Shi, Bai, and Yao 2017; Hu et al. 2020; Du et al. 2022) and length-insensitive LISTER (Cheng et al. 2023). They do not perform well on short text recognition although exhibiting slightly stronger capability in long text recognition.

SMTR circumvents the above problems and recognizes text by sub-string matching. This scheme ensures SMTR’s applicability to long text even when only seen short text images, as sub-string is an essential component for both short and long text.

## 3 Method

Fig. 2 illustrates the overall architecture of SMTR. Given a text image  $X \in \mathbb{R}^{3 \times H \times W}$ , the image encoder extracts its image embeddings  $E_I$ . A sub-string (S) is encoded into both next and previous queries ( $Q_n$  and  $Q_p$ ) by the sub-string encoder.  $Q_n$  and  $Q_p$  are then fed into the sub-string matcher, which implicitly matches the sub-string in the text image and recognizes its next and previous characters bidirectionally. In addition, we discuss issues raised within this new string-matching-based paradigm and propose our solutions.

### 3.1 Image Encoder

To accommodate various aspect ratios of the input  $X$ , we develop a dedicated image encoder termed FocalSVTR to extract visual features as in LISTER (Cheng et al. 2023). Firstly, the input  $X$  is divided into patch embeddings ( $\in \mathbb{R}^{C_0 \times \frac{H}{4} \times \frac{W}{4}}$ ) by two convolution with stride 2. Then, following SVTR (Du et al. 2022), three stages comprising [6, 6, 6] layers of focal modulation (Awais et al. 2023) are stacked. At the end of the first and second stages,  $C_0$  is extended with a factor of 2 by a convolution. In particular, at the end of the second stage, the convolution downsamples the height

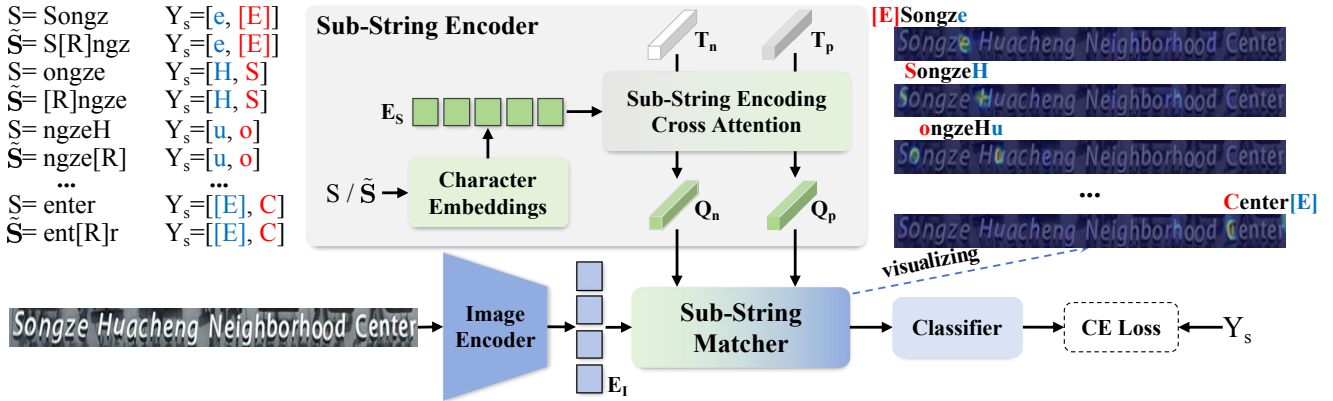


Figure 2: Overview of SMTR. SMTR is a lightweight recognizer consisting of two cross-attention-based modules, i.e., sub-string encoder and sub-string matcher.  $S$  and  $\tilde{S}$  denote a sub-string and its regularized counterpart.  $Y_s$  denotes the next-previous character set of the sub-string.  $[R]$  denotes a randomly selected character from the character set.  $E_s$  and  $E_I$  mean sub-string and image embeddings, respectively.

of the patch embeddings to  $\frac{H}{8}$ . Finally, the output features ( $\in \mathbb{R}^{C \times \frac{H}{8} \times \frac{W}{4}}$ ) are flattened to obtain image embeddings  $E_I \in \mathbb{R}^{C \times \frac{HW}{32}}$ , where  $C = 4C_0$ .

### 3.2 Sub-String Encoder

**Sub-String and Label Generation** For a labeled text image, all sub-strings  $S$  and their next-previous character sets  $Y_s = [Y_n, Y_p]$  can be generated as follows. Taking “datours” in Fig. 4 as an example. It is first prefixed and suffixed with “[B] $_{l_s}$ ”, resulting in the formatted label: “[B] $_{l_s}$  datours[B] $_{l_s}$ ”. Here, “[B] $_{l_s}$ ” represents a string with  $l_s$  blank characters [B], and  $l_s$  is the predefined sub-string length. After that, the formatted label is traversed by a window of size  $l_s$  to obtain all sub-strings and their  $Y_s$  labels. If a sub-string contains [B] on one side, the corresponding label in  $Y_s$  is replaced with [P], indicating that there is no additional character on that side.

Fig. 4 shows all sub-strings of “datours” and their corresponding  $Y_s$  when  $l_s$  is set to 5. The sub-string is initialized with “[B] $_5$ ” and  $Y_s = [d, s]$ , indicating the start of the next and previous inference. For a text of length  $L$ , the number of sub-strings is  $2L + 1$  when  $L < l_s$ , and  $L + l_s$  otherwise.

**Sub-String Encoding** Given a sub-string  $S$ , we employ a lightweight encoding scheme to obtain its feature embedding, the next and previous queries as follows. First, each character in  $S$  is converted into a  $C$ -dim embedding is obtained from a character embedding layer, and the sub-string embedding  $E_s \in \mathbb{R}^{l_s \times C}$  is obtained by feature concatenation. Then, the next token  $T_n \in \mathbb{R}^{1 \times C}$  is introduced, which is a shared and learnable token.  $T_n$  acts as a query and performs cross-attention with  $E_s$ , obtaining the next query  $Q_n \in \mathbb{R}^{1 \times C}$ . Similarly, the previous token  $T_p \in \mathbb{R}^{1 \times C}$  is introduced and generates the previous query  $Q_p \in \mathbb{R}^{1 \times C}$ . The above process can be formulated as:

$$Q_z = \sigma \left( \frac{(T_z W^q)(E_s W^k)^t}{\sqrt{C}} \right) (E_s W^v) + T_z \quad (1)$$

where  $W^q, W^k, W^v \in \mathbb{R}^{C \times C}$  are learnable weights,  $z$  is  $n$  or  $p$ , and  $\sigma$  is softmax function.

### 3.3 Sub-String Matcher

With both image and sub-string embeddings, a direct matching way is to predict the sub-string’s position index through feature interaction. However, this might be less effective to long text due to only trained on short text, as seen in previous methods using absolute positional embeddings (Yue et al. 2020; Yu et al. 2020; Bautista and Atienza 2022).

To circumvent this limitation, we propose a sub-string matcher module that employs adjacent characters  $Y_s$  instead of the absolute position as the prediction targets. The matcher first matches the sub-string within the text image, and then uses the next and previous queries to predict its left and right characters. It gets rid of the global-level absolute positioning and regardless of the text length, concentrating solely on whether the local information within the image matches the sub-string’s embedding. We use the multi-head attention mechanism (Vaswani et al. 2017) to implement this, where  $Q_n$  or  $Q_p$  as query and image embeddings  $E_I$  as key and value. Assuming there are  $h$  attention heads, each with different weight matrices  $W_i^q, W_i^k, W_i^v \in \mathbb{R}^{C \times C_h}$ ,  $i$  denotes the index of the attention head and  $C_h = \frac{C}{h}$ . The matching process can be expressed as:

$$\begin{aligned} \text{Matcher}(Q, E_I) &= \text{MHead}(Q, E_I, E_I) \\ \text{MHead}(Q, K, V) &= \text{Concat}(\text{head}_1, \text{head}_2, \dots, \text{head}_h) \\ \text{head}_i &= A_i(VW_i^v) \\ A_i &= \sigma \left( \frac{(QW_i^q)(KW_i^k)^t}{\sqrt{C_h}} \right) \in \mathbb{R}^{1 \times \frac{HW}{32}} \end{aligned} \quad (2)$$

Taking  $Q_n$  as an example, the sub-string matcher computes the attention map  $A_i$  of  $Q_n$  and  $E_I$ , which focuses on the position of the next character of the sub-string, as shown in the attention maps in Fig. 2. Consequently, the output of the sub-string matcher represents the next character feature ( $\text{Matcher}(Q_n, E_I) \in \mathbb{R}^{1 \times C}$ ), which then un-

dergoes a Classifier ( $\in \mathbb{R}^{C \times (N_c+1)}$ ) to generate prediction  $\tilde{Y}_n \in \mathbb{R}^{1 \times (N_c+1)}$ , i.e.,  $\tilde{Y}_n = \text{Classifier}(\text{Matcher}(Q_n, E_I))$ , where +1 is for the special character [E]. In the same way, the previous character prediction is obtained by  $\tilde{Y}_p = \text{Classifier}(\text{Matcher}(Q_p, E_I))$ .

### 3.4 Optimization Objective

During training, for a text instance with  $N$  sub-strings, SMTR predicts the next and previous characters ( $\tilde{Y}_n$  and  $\tilde{Y}_p$ ) for each sub-string. The loss  $\mathcal{L}$  is computed by comparing the label  $Y_s = [Y_n, Y_p]$  with  $\tilde{Y}_s = [\tilde{Y}_n, \tilde{Y}_p]$ :

$$\mathcal{L} = \frac{1}{K} \sum_{i=1}^N (ce(\sigma(\tilde{Y}_n^i), Y_n^i) + ce(\sigma(\tilde{Y}_p^i), Y_p^i)) \quad (3)$$

$$ce(\tilde{y}, y) = \begin{cases} -\sum_{c=1}^{N_c} y_c \log(\tilde{y}_c), & y \neq [\text{P}]. \\ 0, & y = [\text{P}]. \end{cases}$$

where label  $[P]$  is not involved in the loss computation,  $K$  is the number of valid loss terms. It is equal to  $2N - 2L$  when  $L < l_s$ , and  $2N - 2(l_s - 1)$  otherwise.

### 3.5 Regularization Training

SMTR performs matching and recognition by aligning the sub-string embedding within the image feature space. However, this process can be compromised by similar or repeated sub-strings, as they have quite similar visual features. We categorize this problem as similar sub-string distraction and repeated sub-string confusion, and propose two strategies to alleviate them accordingly. The first is regularization training for similar sub-string distraction described as follows.

SMTR is easily disturbed by sub-strings with similar visual appearance and generates error recognition. As shown in Fig. 3(a), the next character after sub-string “plon.” is mistakenly identified as a similar sub-string “sion.”, resulting in an undesired circular recognition.

To overcome this issue, SMTR should be endowed with the ability to discover subtle differences between similar sub-strings. Motivated by this, we propose regularization training (RT), which alleviates this problem by generating similar sub-strings  $\tilde{S}$  for  $S$  for training reinforcement. As depicted in the top-left side of Fig. 2, one character in  $S$  is replaced with [R], a character randomly selected from the character set, to obtain  $\tilde{S}$ , and keep its label  $Y_s$  unchanged. By doing this, the number of similar sub-strings is largely enriched during training. SMTR is compelled to leverage all the  $l_s$  characters, rather than a few nearby ones, to distinguish similar sub-strings appearing in the same text image, which therefore can be better identified. As seen in Fig. 3(b), attention maps are correctly displayed and the instance is well recognized when RT is considered.

### 3.6 Inference Augmentation

We then introduce the inference augmentation (IA) proposed to mitigate the repeated sub-string confusion as follows.

During the inference phase, it cannot obtain all the sub-strings in the image directly. Therefore, we implement the

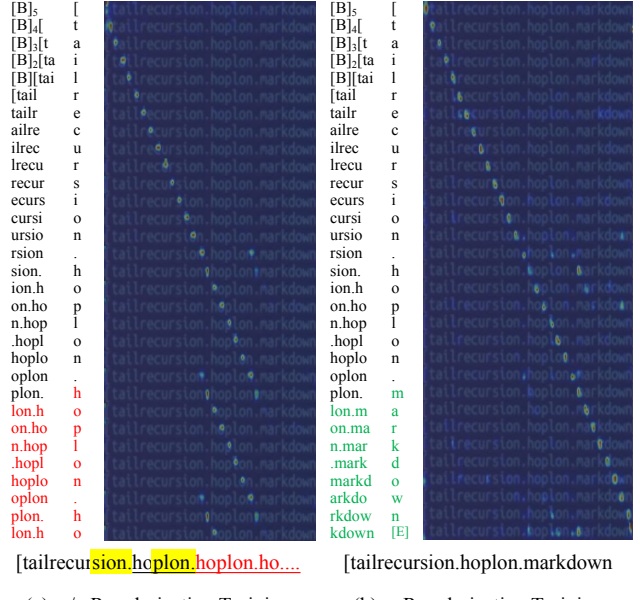


Figure 3: Attention maps of SMTR w/o (left) and w (right) the proposed regularization training, which rectifies recognition errors (red) caused by similar sub-strings (yellow).

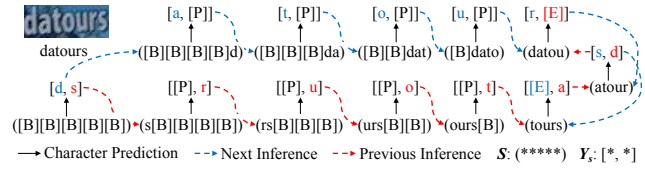


Figure 4: Illustration of SMTR base inference process, where [E] means the end token for inference termination.

base inference by decoding iteratively: the next and previous tokens ( $T_n, T_p \in \mathbb{R}^{1 \times C}$ ) are generated and fed into SMTR to iteratively predict the next and previous characters as shown in Fig. 4. The process is terminated when the end token [E] is predicted. Alg. 1 provides a detailed description of this process.

The base inference fails to distinguish repeated sub-strings in one image, such as the *SMTR w/o IA* result in Fig. 5 and Fig. 12 in Supplementary. Tab. 1 shows the statistics of repeated sub-strings in typical short text datasets and LTB. The high percentage of repeated sub-strings (near 10%) seriously affects the recognition. Consequently, we propose IA that first slices the long text image into three short sub-images and then employs a split-merge scheme for recognition. This process is depicted in Fig. 5 and summarized in Alg. 2 in Supplementary. Specifically, the text image is sliced into three sub-images whose width is halved, i.e., the left sub-image  $\text{Img1}$ , the right sub-image  $\text{Img2}$  and the central sub-image  $\text{Img3}$ . Note that both  $\text{Img1}$  and  $\text{Img2}$  are overlapped with  $\text{Img3}$ . Then, by taking advantage of the bidirectional recognition property of SMTR, we recognize  $\text{Img1}$  and  $\text{Img2}$  following the next and previous pre-

---

**Algorithm 1:** Pseudo-code of Base Inference in Python.

---

```

def Inference(Img, Tok, Ss=[0]*ls, Se=[]):
    # Img: Input Image,  $3 \times H \times W$ .
    # Tok: Next or Previous Token,  $1 \times C$ .
    # Ss/Se: The start/end sub-string.
    # [0]: The [B].
    # ls: The length of sub-string.
    Result = [], S = Ss
    IE = ImageEncoder(Img) #  $\frac{HW}{32} \times C$ 
    While True:
        Q = SubStringEncoder(Tok, S)
        O = SubStringMatcher(Q, IE)
        Char = Classifier(O).argmax(-1)
        if Tok is  $T_n$ :
            S = S[1:] + [Char]
        else:
            S = [Char] + S[:1]
        # EOS: The index of end symbol.
        if Char == EOS or S == Se:
            break
        Result.append(Char)
    return Result
    # Result is the recognition result.

```

---

Dataset	Samples	Repeat $S$	
Union14M-L Training	3,230,742	885	0.03%
Union14M-L Benchmarks	409,383	22	0.01%
Common Benchmarks	7,248	0	0.00%
LTB	4,789	472	9.86%
LTB with IA	4,789	20	0.42%

Table 1: The percentage of text instances with repeated sub-strings ( $l_s \geq 5$ ) in different datasets. Inference augmentation (IA) drastically reduces the percentage in LTB.

dition paths, respectively, i.e.,  $\text{Inference}(\text{Img}_1, T_n)$  and  $\text{Inference}(\text{Img}_2, T_p)$ . The process obtains the results shown in the top line of Fig. 5 in roughly half of the inference iterations, as both predictions can be carried out in parallel. Since the slice may operate on characters and lead to mis-recognition, we pick out recognized sub-strings also appearing in  $\text{Img}_3$  from both sides according to attention maps (highlighted by yellow in Fig. 5), i.e.,  $S_s$  and  $S_e$ . In the following, we predict  $\text{Img}_3$  with  $\text{Inference}(\text{Img}_3, T_n, S_s, S_e)$ , which gets the central characters. Finally, the full result, e.g., the *SMTR w IA* result in Fig. 5, is obtained by a simple post-processing.

It is seen in Tab. 1 that IA drastically reduces the percentage of repeated sub-strings in LTB from nearly 10% to 0.4%, thus significantly alleviating the repeated sub-string confusion. Meanwhile, the devised split-merge recognition scheme robustly recognizes long text images. The effectiveness of IA is demonstrated in Tab. 4 and Fig. 6.

### 3.7 Long Text Benchmark

Existing public benchmarks mainly focus on short text recognition and their instances predominantly consist of text with no more than 25 characters. However, they also have



Figure 5: Illustration of inference augmentation (IA) for long text recognition. Text spaces are manually inserted.

Source	Train	Test	Source	Train	Test
RCTW (2017)	173	1	MTWI (2018)	516	77
LSVT (2019)	968	111	UberText (2017)	465	40
ArT (2019)	28	4	COCOText (2016)	23	0
IntelOCR (2021)	792	111	ReCTS (2019)	3	1
TextOCR (2021)	140	16	KAIST (2011)	11	0
HierText (2022)	572	82	NEOCR (2012)	59	10
MLT19 (2019)	25	1	CTW1500 (2017)	551	0
IIIT-ILST (2017)	1	0	<b>Total</b>		4,789

Table 2: Composition details of LTB.

a few instances with more than 25 characters. These instances are usually regarded as noise and discarded in developing traditional short text models. Here, we collect these instances and construct a Long Text Benchmark (LTB). LTB contains nearly 4.8k text whose length is above 25. The composition of LTB is detailed in Tab. 2. Since all samples are excluded from the training process, LTB establishes a new benchmark exclusively for evaluating the performance of STR models on long text recognition. To assess the impact of length variation on recognition, we divide LTB into three parts based on text length: [26-35], [36-55], and  $\geq 56$ . The results of typical STR methods and SMTR are presented in Fig. 1 and Tab. 4, which will be discussed later.

## 4 Experiments

### 4.1 Datasets and Implementation Details

We evaluate SMTR on both English and Chinese datasets. For English, our models are trained on Union14M-L (Jiang et al. 2023), which contains about 4 million real-world text images ( $L \leq 25$ ). Then, the models are tested on both LTB and two short text benchmarks: (1) Common benchmarks, i.e., ICDAR 2013 (IC13) (KaratzasAU et al. 2013), Street View Text (SVT) (Wang, Babenko, and Belongie 2011), IIIT5K-Words (IIIT) (Mishra, Karteek, and Jawahar 2012), ICDAR 2015 (IC15) (Karatzas et al. 2015), Street View Text-Perspective (SVTP) (Phan et al. 2013) and CUTE80 (CUTE) (Anhar et al. 2014). For IC13 and IC15, we use the versions with 857 and 1,811 images, respectively. (2) Union14M benchmark, which includes seven challenging subsets: Curve (CUR), Multi-Oriented (MLO), Artistic (ART), Contextless (CTL), Salient (SAL), Multi-Words (MLW) and General (GEN). For Chinese, we use Chinese text recognition (CTR) dataset (Chen et al. 2021), which contains four subsets: Scene, Web, Document (*Doc*) and Hand-Writing (*HW*). We train the model on the whole train-

$\tilde{S}$	$l_s$	Common	U14M	LTB	Avg
w/o	5	95.65	83.58	32.30	70.51
	1	95.94	84.14	44.37	74.82
2	4	<b>96.04</b>	84.51	45.24	75.26
	5	95.90	<b>85.00</b>	<b>47.00</b>	<b>75.97</b>
	6	95.64	84.26	45.06	74.99
	7	95.77	83.80	40.55	73.37

Table 3: Ablation study on regularization training and  $l_s$ .

Method	$L_{[26,35]}$ 3376	$L_{[36,55]}$ 1147	$L_{\geq 56}$ 266	W-Avg	A-Avg
FocalSVTR	51.04	25.37	0.38	42.08	25.59
sinAR	25.53	0.00	0.00	18.00	8.51
PARSeq (2022)	0.00	0.00	0.00	0.00	0.00
LISTER (2023)	51.16	26.59	2.26	42.56	26.67
SMTR w/o IA	53.06	37.05	13.16	47.00	34.42
SMTR	<b>55.48</b>	<b>43.68</b>	<b>25.56</b>	<b>50.99</b>	<b>41.57</b>

Table 4: Model comparing results on LTB. sinAR uses an autoregressive decoder with sinusoidal position encoding.

ing set and use Scene validation subset to determine the best model, which is then assessed on the test subsets.

We use AdamW optimizer (Loshchilov and Hutter 2019) with a weight decay of 0.05 for training. The LR is set to  $6.5 \times 10^{-4}$  and batchsize is set to 1024. One cycle LR scheduler (I. Loshchilov and Hutter 2017) with 1.5/4.5 epochs linear warm-up is used in all the 20/100 epochs, where a/b means a for English and b for Chinese. Preserving the aspect ratio, all of images are resized to a maximum pixel size of  $32 \times 128$  if aspect ratio is less than 4, otherwise, resized to  $H = 32$  and  $W$  up to 384. Word accuracy is used as the evaluation metric. Data augmentation like rotation, perspective distortion, motion blur and gaussian noise, are randomly performed and the maximum text length is set to 25 during training. The size of the character set  $N_c$  is set to 96 for English and 6625 (Li et al. 2022) for Chinese. All models are trained with mixed-precision on 4 RTX 3090 GPUs.

## 4.2 Ablation Study

**Effectiveness of Regularization Training (RT)** As shown in Fig. 3(b), RT mitigates the sub-string mismatching well. With RT, SMTR effectively discriminates two similar sub-strings (“sion.” and “plon.”) and recognizes the text accurately. Tab. 3 quantifies the effectiveness of RT. It takes effects for both short and long text, where a notable 12.07% accuracy improvement is observed on LTB. The result indicates similar sub-strings are much better identified.

Tab. 3 also ablates  $l_s$  and  $\tilde{S}$ , the number of regularized sub-strings. The results indicate that  $l_s > 5$  is not necessary. In addition, increasing  $\tilde{S}$  enhances the accuracy of both short and long text, again validating the positive effect of RT.

**Effectiveness of Inference Augmentation (IA)** We evaluated IA from both accuracy and efficiency aspects. As shown in Tab. 4, IA largely improves the accuracy of SMTR on LTB, with weighted (W-Avg) and arithmetic (A-Avg) av-

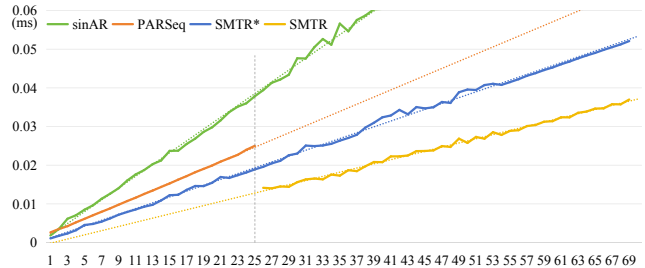


Figure 6: Inference speeds of different methods. SMTR\* means not using inference augmentation. For a fair comparison, the same encoder is employed for all the methods and only time consumption of the decoding stage is considered.

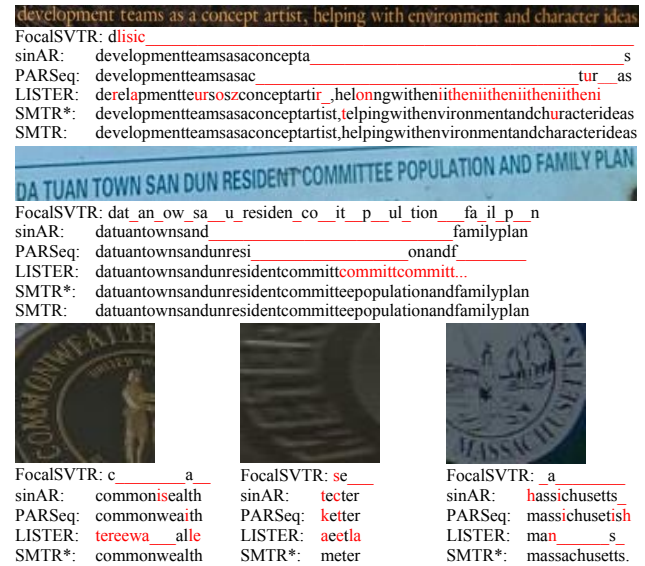


Figure 7: Illustration of the predictions of two long text images from LTB and three short text images from Union14M Benchmarks. In addition, their attention maps are visualized in Supplementary for qualitative analysis.

erage increasing by 3.99% and 7.17%, respectively. Notably, accuracy gains from IA become more distinct as the text length increases, where 2.42%, 6.63%, and 12.4% improvements are observed across the three subsets. The results can be explained as the higher likelihood of repeating sub-strings with text length increases. Regarding the inference speed, as illustrated in Fig. 6, IA enhances SMTR’s efficiency in long text recognition substantially. This improvement is mainly due to IA’s split-merge processing, which reduces the iterations in long text recognition remarkably.

**Comparison with existing methods on LTB** As aforementioned, current STR models, despite being designed for short text recognition, some of them can still recognize long text to some extent, e.g., CTC-based and autoregressive decoding ones. To ensure a fair comparison with them, we set an experiment by uniformly adopting FocalSVTR as the image encoder, keeping their decoders unchanged, and retrain-

Method	Common Benchmarks								Union14M-L Benchmarks								Params ( $\times 10^6$ )
	IC13	SVT	IIIT	IC15	SVTP	CUTE	Avg	CUR	MLO	ART	CTL	SAL	MLW	GEN	Avg		
RoScanner (2020)	95.7	92.4	96.8	86.4	83.9	93.8	91.50	66.2	54.2	61.4	72.7	60.1	74.2	75.7	66.36	0.0	48.0
SRN (2020)	94.7	89.5	95.5	79.1	83.9	91.3	89.00	49.7	20.0	50.7	61.0	43.9	51.5	62.7	48.50	0.0	54.7
VisionLAN (2021)	95.1	91.3	96.3	83.6	85.4	92.4	90.68	70.7	57.2	56.7	63.8	67.6	47.3	74.2	62.50	0.0	32.8
SVTR-B (2022)	97.5	96.4	97.8	89.3	91.0	96.2	94.72	85.4	87.4	68.9	79.5	84.3	79.1	81.8	80.91	0.0	24.6
PARSeq (2022)	97.9	98.1	<b>99.0</b>	90.0	94.5	97.6	96.18	88.4	89.2	<b>78.1</b>	<b>84.0</b>	82.6	86.6	84.7	84.79	0.0	17.0
CRNN (2017)	91.8	83.8	90.8	71.8	70.4	80.9	81.58	19.4	4.5	34.2	44.0	16.7	35.7	60.4	30.70	-	8.3
ASTER (2019)	92.6	88.9	94.3	77.7	80.5	86.5	86.75	38.4	13.0	41.8	52.9	31.9	49.8	66.7	42.07	-	27.2
NRTR (2019)	96.9	94.0	96.2	80.9	84.8	92.0	90.80	49.3	40.6	54.3	69.6	42.9	75.5	75.2	58.20	-	31.7
SAR (2019)	96.0	92.4	96.6	82.0	85.7	92.7	90.90	68.9	56.9	60.6	73.3	60.1	74.6	76.0	67.20	-	57.7
ABINet (2021)	97.2	95.7	97.2	87.6	92.1	94.4	94.03	75.0	61.5	65.3	71.1	72.9	59.1	79.4	69.19	-	36.7
MAERec (2023)	97.6	96.8	98.0	87.1	93.2	<b>97.9</b>	95.10	81.4	71.4	72.0	82.0	78.5	82.4	82.5	78.60	-	35.7
LISTER (2023)	97.4	98.1	98.2	89.2	93.5	95.5	95.33	71.6	55.9	68.9	76.4	68.1	80.2	80.9	71.72	42.6	49.9
OTE (2024)	98.0	98.0	98.1	89.1	<b>95.5</b>	97.6	96.10	83.1	82.8	73.5	73.7	79.7	70.3	82.2	77.90	-	25.2
FocalSVTR	97.3	96.3	98.2	87.4	88.4	96.2	93.97	77.7	62.4	65.7	78.6	71.6	81.3	79.2	73.80	42.1	14.7
sinAR	98.1	<b>98.3</b>	<b>99.0</b>	89.8	94.2	<b>97.9</b>	<b>96.22</b>	88.1	<b>91.2</b>	76.2	83.3	83.2	85.6	<b>84.9</b>	84.62	18.0	19.3
<b>SMTR</b>	<b>98.3</b>	97.4	<b>99.0</b>	<b>90.1</b>	92.7	<b>97.9</b>	95.90	<b>89.1</b>	87.7	76.8	83.9	<b>84.6</b>	<b>89.3</b>	83.7	<b>85.00</b>	<b>51.0</b>	15.8

Table 5: Results on short text benchmarks and LTB tested against existing models. - means the model cannot be used to recognize long text directly.

ing the models using the same hyper-parameters presented in section 4.1. Tab. 4 and Tab. 5 give the results, where FocalSVTR is the encoder appending with a CTC decoder, sinAR is a variant of NRTR (Sheng, Chen, and Xu 2019).

As seen in Tab. 4, SMTR consistently outperforms the compared models in terms of accuracy, and their gaps are sharply enlarged as the text length increases. When inspecting the arithmetic average for  $L > 35$ , SMTR outperforms FocalSVTR, sinAR and LISTER by 15.98%, 33.06%, and 14.90%, respectively. The first two long text examples in Fig. 7 show that all four comparing methods suffer from the problem of missing characters. In addition, sinAR and PARSeq are only able to recognize the front characters due to employing absolute positional encoding and only trained on short text. LISTER encounters the problem of circular recognition due to capturing incorrect neighbor characters. In contrast, SMTR effectively recognizes these instances by sub-string matching. These results convincingly verify the superiority of SMTR in recognizing long text and addressing the OOL challenge. Attention maps of the two instances are provided in Supplementary.

### 4.3 Comparison with State-of-the-arts

**Results on English Benchmarks.** We apply SMTR to Common benchmarks, Union14M benchmarks and LTB, and compare it with existing STR models. The results are in Tab. 5. Compared with PARSeq, one leading method in short text benchmarks, SMTR exhibits quite similar accuracy. In addition, it correctly recognizes half of LTB text, which is incapable for PARSeq. Note that sinAR also achieves very competitive results on short text benchmarks. However, its weak extrapolation capability restricts the performance on LTB. On the other hand, FocalSVTR performs decent on short text benchmarks, but on LTB it performs on par with LISTER, which is a dedicated model for long text recognition. The results above basically verify our assessment in

Fig. 1. To sum, by adopting a novel sub-string matching-based recognition paradigm, SMTR well recognizes both short and long text, which would be a promising property for many STR-related applications.

In the bottom of Fig. 7 we also present the recognition of three challenging short text images. CTC-based FocalSVTR and LISTER show severe mis-recognition due to their reliance on a priori of regular text. In contrast, sinAR and PARSeq can recognize a majority of the text, encountering errors only when dealing with particularly challenging characters. SMTR\* (the same as SMTR when recognizing short text) accurately identifies all the characters, showing robustness in handling challenging short text.

**Results on Chinese Benchmark.** The OOL challenge is pervasive across languages. To verify the multilingual adaptability of SMTR, we conduct evaluations on the Chinese text recognition benchmark (CTR) (Chen et al. 2021). In line with CCR-CLIP (Yu et al. 2023), SMTR refrains from utilizing data augmentation (w/o Aug) to ensure a fair comparison. As presented in Tab. 6, SMTR outperforms LISTER by 6.83% on *Scene* subset. Note that SMTR gets this result without training on long text while LISTER has no imposed length limitation during training. Despite this discrepancy, SMTR still maintains an accuracy gain of 10.61% over LISTER in Chinese long text, as depicted in Tab. 7. Meanwhile, SMTR achieves a new state-of-the-art on CTR, boosting an accuracy gain of 5.55% compared to CCR-CLIP, the previous best method. SMTR’s performance can be further improved with data augmentation. These results demonstrate SMTR’s great adaptability in multilingual recognition.

## 5 Conclusion

In this paper, we observe that, in real applications, STR models sometimes have to recognize long text images and existing models trained on short text images cannot accomplish

Method	Scene	Web	Doc	HW	Avg	Params $\times 10^6$
CRNN (2017)	53.4	57.0	96.6	50.8	64.45	12.4
ASTER (2019)	61.3	51.7	96.2	37.0	61.55	27.2
MORAN (2019)	54.6	31.5	86.1	16.2	47.10	28.5
SAR (2019)	59.7	58.0	95.7	36.5	62.48	27.8
SEED (2020)	44.7	28.1	91.4	21.0	46.30	36.1
MASTER (2021)	62.8	52.1	84.4	26.9	56.55	62.8
ABINet (2021)	66.6	63.2	98.2	53.1	70.28	53.1
TransOCR (2021)	71.3	64.8	97.1	53.0	71.55	83.9
SVTR-B (2022)	71.7	73.8	98.2	52.2	73.98	26.3
CCR-CLIP (2023)	71.3	69.2	98.3	60.3	74.78	62.0
LISTER (2023)	73.0	-	-	-	-	55.0
SMTR w/o Aug	79.8	80.6	99.1	61.9	80.33	20.8
SMTR w Aug	<b>83.4</b>	<b>83.0</b>	<b>99.3</b>	<b>65.1</b>	<b>82.68</b>	20.8

Table 6: Results on CTR dataset comparing existing models.

Method	$L_{\leq 25}$	$L_{> 25}$	Weighted	Arithmetic
	63136	510	Avg	Avg
LISTER (2023)	73.00	35.00	72.69	54.00
SMTR	79.83	45.61	79.56	62.74

Table 7: Short and long text recognition results on *Scene*.

this task well. We term this the OOL challenge. We construct the LTB dataset for long text recognition assessment, and propose a novel SMTR that employs a sub-string-matching-based paradigm to overcome this challenge. SMTR implements the recognition by iteratively predicting the next and previous characters of a sub-string. It is capable of recognizing both short and long text. To make the recognition effective in this new paradigm, we introduce regularization training to suppress distractions caused by similar sub-strings, and inference augmentation to alleviate confusion caused by repeated sub-strings and improve recognition efficiency. Experimental results show that SMTR not only surpasses existing methods by a clear margin on LTB, but is also highly competitive on challenging short text benchmarks. Nevertheless, SMTR employs an iterative recognition paradigm in inference thus the speed is not fast. Hence, our future research will be devoted to addressing this problem.

## References

Anhar, R.; Palaiahnakote, S.; Chan, C. S.; and Tan, C. L. 2014. A robust arbitrary text detection system for natural scene images. *Expert Syst. Appl.*, 41(18): 8027–8048.

Awais, M.; Naseer, M.; Khan, S.; Anwer, R. M.; Cholakkal, H.; Shah, M.; Yang, M.-H.; and Khan, F. S. 2023. Foundational models defining a new era in vision: A survey and outlook. *CoRR*, abs/2307.13721.

Bautista, D.; and Atienza, R. 2022. Scene Text Recognition with Permuted Autoregressive Sequence Models. In *ECCV*, 178–196.

Chen, J.; Li, B.; and Xue, X. 2021. Scene Text Telescope: Text-Focused Scene Image Super-Resolution. In *CVPR*, 12021–12030.

Chen, J.; Yu, H.; Ma, J.; Guan, M.; Xu, X.; Wang, X.; Qu, S.; Li, B.; and Xue, X. 2021. Benchmarking Chinese Text Recognition: Datasets, Baselines, and an Empirical Study. *CoRR*, abs/2112.15093.

Cheng, C.; Wang, P.; Da, C.; Zheng, Q.; and Yao, C. 2023. LISTER: Neighbor Decoding for Length-Insensitive Scene Text Recognition. In *ICCV*, 19484–19494.

Chng, C.; Liu, Y.; Sun, Y.; Ng, C.; Luo, C.; N.; Fang, C.; Zhang, S.; Han, J.; Ding, E.; et al. 2019. ICDAR2019 robust reading challenge on arbitrary-shaped text-rrc-art. In *ICDAR*, 1571–1576.

Chung, J.; Gülcöhre, C.; Cho, K.; and Bengio, Y. 2014. Empirical Evaluation of Gated Recurrent Neural Networks on Sequence Modeling. *CoRR*, abs/1412.3555.

Du, Y.; Chen, Z.; Jia, C.; Yin, X.; Li, C.; Du, Y.; and Jiang, Y. 2023. Context Perception Parallel Decoder for Scene Text Recognition. *CoRR*, abs/2307.12270.

Du, Y.; Chen, Z.; Jia, C.; Yin, X.; Zheng, T.; Li, C.; Du, Y.; and Jiang, Y. 2022. SVTR: Scene Text Recognition with a Single Visual Model. In *IJCAI*, 884–890.

Du, Y.; Chen, Z.; Su, Y.; Jia, C.; and Jiang, Y. 2024. Instruction-Guided Scene Text Recognition. *CoRR*, abs/2401.17851.

Fang, S.; Xie, H.; Wang, Y.; Mao, Z.; and Zhang, Y. 2021. Read Like Humans: Autonomous, Bidirectional and Iterative Language Modeling for Scene Text Recognition. In *CVPR*, 7098–7107.

Graves, A.; Fernández, S.; Gomez, F.; and Schmidhuber, J. 2006. Connectionist Temporal Classification: Labelling Unsegmented Sequence Data with Recurrent Neural Networks. In *ICML*, 369–376.

Gupta, A.; Vedaldi, A.; and Zisserman, A. 2016. Synthetic Data for Text Localisation in Natural Images. In *CVPR*, 2315–2324.

He, M.; Liu, Y.; Yang, Z.; Zhang, S.; Luo, C.; Gao, F.; Zheng, Q.; Wang, Y.; Zhang, X.; and Jin, L. 2018. ICPR2018 contest on robust reading for multi-type web images. In *ICPR*, 7–12.

Hochreiter, S.; and Schmidhuber, J. 1997. Long Short-Term Memory. *Neural Comput.*, 9(8): 1735–1780.

Hu, W.; Cai, X.; Hou, J.; Yi, S.; and Lin, Z. 2020. GTC: Guided training of ctc towards efficient and accurate scene text recognition. In *AAAI*, 11005–11012.

Jaderberg, M.; Simonyan, K.; Vedaldi, A.; and Zisserman, A. 2014. Synthetic Data and Artificial Neural Networks for Natural Scene Text Recognition. *CoRR*, abs/1406.2227.

Jiang, Q.; Wang, J.; Peng, D.; Liu, C.; and Jin, L. 2023. Revisiting Scene Text Recognition: A Data Perspective. In *ICCV*, 20486–20497.

Jung, J.; Lee, S.; Cho, M.; and Kim, J. 2011. Touch TT: Scene text extractor using touchscreen interface. *ETRI*, 78–88.

Karatzas, D.; Gomez-Bigorda, L.; Nicolaou, A.; Ghosh, S.; Bagdanov, A.; Iwamura, M.; Matas, J.; Neumann, L.; Chandrasekhar, V. R.; Lu, S.; Shafait, F.; Uchida, S.; and Valveny,

E. 2015. ICDAR 2015 competition on Robust Reading. In *ICDAR*, 1156–1160.

KaratzasAU, D.; ShafaitAU, F.; UchidaAU, S.; IwamuraAU, M.; i. BigordaAU, L. G.; MestreAU, S. R.; MasAU, J.; MottaAU, D. F.; AlmazànAU, J. A.; and de las Heras, L. P. 2013. ICDAR 2013 Robust Reading Competition. In *ICDAR*, 1484–1493.

Krylov, I.; Nosov, S.; and Sovrasov, V. 2021. Open images v5 text annotation and yet another mask text spotter. In *Asian Conference on Machine Learning*, 379–389. PMLR.

Lee, C.; and Osindero, S. 2016. Recursive recurrent nets with attention modeling for ocr in the wild. In *CVPR*, 2231–2239.

Li, C.; Liu, W.; Guo, R.; Yin, X.; Jiang, K.; Du, Y.; Du, Y.; Zhu, L.; Lai, B.; Hu, X.; Yu, D.; and Ma, Y. 2022. PP-OCRv3: More Attempts for the Improvement of Ultra Lightweight OCR System. *CoRR*, abs/2206.03001.

Li, H.; Wang, P.; Shen, C.; and Zhang, G. 2019. Show, attend and read: A simple and strong baseline for irregular text recognition. In *AAAI*, 8610–8617.

Liu, Y.; Jin, L.; Zhang, S.; and Zhang, S. 2017. Detecting curve text in the wild: New dataset and new solution. *CoRR*, abs/1712.02170.

Long, S.; Qin, S.; Pantelev, D.; Bissacco, A.; Fujii, Y.; and Raptis, M. 2022. Towards end-to-end unified scene text detection and layout analysis. In *CVPR*, 1049–1059.

Loshchilov, I.; and Hutter, F. 2019. Decoupled Weight Decay Regularization. In *ICLR*.

Lu, N.; Yu, W.; Qi, X.; Chen, Y.; Gong, P.; Xiao, R.; and Bai, X. 2021. MASTER: Multi-aspect non-local network for scene text recognition. *Pattern Recognit.*, 117: 107980.

Luo, C.; Jin, L.; and Sun, Z. 2019. MORAN: A Multi-Object Rectified Attention Network for Scene Text Recognition. *Pattern Recognit.*, 90: 109–118.

Mathew, M.; Jain, M.; and Jawahar, C. 2017. Benchmarking scene text recognition in Devanagari, Telugu and Malayalam. In *ICDAR*, volume 7, 42–46.

Mishra, A.; Karteek, A.; and Jawahar, C. V. 2012. Scene Text Recognition using Higher Order Language Priors. In *BMVC*, 1–11.

Nagy, R.; Dicker, A.; and Meyer-Wegener, K. 2012. NEOCR: A configurable dataset for natural image text recognition. In *Camera-Based Document Analysis and Recognition*, 150–163.

Nayef, N.; Patel, Y.; Busta, M.; Chowdhury, P.; Karatzas, D.; Khelif, W.; Matas, J.; Pal, U.; Burie, J.; Liu, C.; et al. 2019. ICDAR2019 robust reading challenge on multilingual scene text detection and recognition—RRC-MLT-2019. In *ICDAR*, 1582–1587.

Phan, T. Q.; Shrivakumara, P.; Tian, S.; and Tan, C. L. 2013. Recognizing Text with Perspective Distortion in Natural Scenes. In *CVPR*, 569–576.

Qiao, Z.; Zhou, Y.; Yang, D.; Zhou, Y.; and Wang, W. 2020. SEED: Semantics Enhanced Encoder-Decoder Framework for Scene Text Recognition. In *CVPR*, 13525–13534.

Sheng, F.; Chen, Z.; and Xu, B. 2019. NRTTR: A No-Recurrence Sequence-to-Sequence Model for Scene Text Recognition. In *ICDAR*, 781–786.

Shi, B.; Bai, X.; and Yao, C. 2017. An End-to-End Trainable Neural Network for Image-Based Sequence Recognition and Its Application to Scene Text Recognition. *IEEE Trans. Pattern Anal. Mach. Intell.*, 39(11): 2298–2304.

Shi, B.; Yang, M.; Wang, X.; Lyu, P.; Yao, C.; and Bai, X. 2019. ASTER: An Attentional Scene Text Recognizer with Flexible Rectification. *IEEE Trans. Pattern Anal. Mach. Intell.*, 41(9): 2035–2048.

Shi, B.; Yao, C.; Liao, M.; Yang, M.; Xu, P.; Cui, L.; Belongie, S.; Lu, S.; and Bai, X. 2017. ICDAR2017 competition on reading chinese text in the wild (rctw-17). In *ICDAR*, 1429–1434.

Singh, A.; Pang, G.; Toh, M.; Huang, J.; Galuba, W.; and Hassner, T. 2021. TextOCR: Towards large-scale end-to-end reasoning for arbitrary-shaped scene text. In *CVPR*, 8802–8812.

Sun, Y.; Ni, Z.; Chng, C.; Liu, Y.; Luo, C.; Ng, C.; Han, J.; Ding, E.; Liu, J.; Karatzas, D.; et al. 2019. ICDAR 2019 competition on large-scale street view text with partial labeling—RRC-LSVT. In *ICDAR*, 1557–1562.

Vaswani, A.; Shazeer, N.; Parmar, N.; Uszkoreit, J.; Jones, L.; Gomez, A.; Kaiser, L.; and Polosukhin, I. 2017. Attention is All you Need. In *NIPS*, 5998–6008.

Veit, A.; Matera, T.; Neumann, L.; Matas, J.; and Belongie, S. 2016. Coco-text: Dataset and benchmark for text detection and recognition in natural images. *CoRR*, abs/1601.07140.

I. Loshchilov; and Hutter, F. 2017. SGDR: Stochastic Gradient Descent with Warm Restarts. In *ICLR*.

Wang, K.; Babenko, B.; and Belongie, S. 2011. End-to-end scene text recognition. In *ICCV*, 1457–1464.

Wang, Y.; Xie, H.; Fang, S.; Wang, J.; Zhu, S.; and Zhang, Y. 2021. From Two to One: A New Scene Text Recognizer With Visual Language Modeling Network. In *ICCV*, 14194–14203.

Xu, J.; Wang, Y.; Xie, H.; and Zhang, Y. 2024. OTE: Exploring Accurate Scene Text Recognition Using One Token. In *CVPR*, 28327–28336.

Yu, D.; Li, X.; Zhang, C.; Liu, T.; Han, J.; Liu, J.; and Ding, E. 2020. Towards accurate scene text recognition with semantic reasoning networks. In *CVPR*, 12113–12122.

Yu, H.; Wang, X.; Li, B.; and Xue, X. 2023. Chinese Text Recognition with A Pre-Trained CLIP-Like Model Through Image-IDS Aligning. In *ICCV*, 11909–11918.

Yue, X.; Kuang, Z.; Lin, C.; Sun, H.; and Zhang, W. 2020. RobustScanner: Dynamically enhancing positional clues for robust text recognition. In *ECCV*, 135–151.

Zhang, B.; Xie, H.; Wang, Y.; Xu, J.; and Zhang, Y. 2023. Linguistic More: Taking a Further Step toward Efficient and Accurate Scene Text Recognition. In *IJCAI*, 1704–1712.

Zhang, R.; Zhou, Y.; Jiang, Q.; Song, Q.; Li, N.; Zhou, K.; Wang, L.; Wang, D.; Liao, M.; Yang, M.; et al. 2019. ICDAR

2019 robust reading challenge on reading chinese text on signboard. In *ICDAR*, 1577–1581.

Zhang, Y.; Gueguen, L.; Zharkov, I.; Zhang, P.; Seifert, K.; and Kadlec, B. 2017. Uber-text: A large-scale dataset for optical character recognition from street-level imagery. In *Scene Understanding Workshop-CVPR*, 5.

Zheng, T.; Chen, Z.; Fang, S.; Xie, H.; and Jiang, Y. 2024. CDistNet: Perceiving multi-domain character distance for robust text recognition. *Int. J. Comput. Vis.*, 132(2): 300–318.

**Algorithm 2:** Pseudo-code of Inference Augmentation.

```

def InferenceLongText (Img):
    # Img: Input Image,  $3 \times H \times W$ .
    Img1, Img2, Img3 = Slice(Img)
    R1 = Inference(Img1,  $T_n$ )
    #  $[::-1]$  for inverted a list.
    R2 = Inference(Img2,  $T_p$ )  $[::-1]$ 
     $T_{Next} = R1[:- (l_s + 1)]$ 
     $T_{Pre} = R2[l_s + 1:]$ 
    Ss = R1 $[- (l_s + 1) :- 1]$ 
    Se = R2 $[1: l_s + 1]$ 
    R3 = Inference(Img3,  $T_n$ , Ss, Se)
     $T_{Mid} = R3[:- (l_s - 1)]$ 
    Result =  $T_{Next} + Ss + T_{Mid} + Se + T_{Pre}$ 
    return Result
    # Result is the recognition.

```

## A Inference Augmentation

Algorithm 2 presents the implementation details of inference augmentation in Python style. Specifically, the `Slice` operation splits a image into three sub-images as shown in Fig. 4 of the main script. This is followed by bi-directional inference using `Inference` to obtain recognition results for `Img1` and `Img2`. The subsequent correction of misrecognition caused by `Slice` is performed on `Img3`. Finally, with a straightforward post-processing step, the result of long text recognition is obtained. The operation `Inference` is detailed in Algorithm 1 of the main script.

## B Impact of $h$ , residual and MLP

As shown in Tab. 8, residual and MLP exhibit effectiveness in short text recognition no matter how the head number ( $h$ ) is set to either 2 or 12. However, an inverse result is evident in long text recognition. When the residual is applied,  $\tilde{Y}_n$  is adapted as  $\text{Classifier}(\text{Matcher}(Q_n, E_I) + Q_n)$ . This suggests that the content of a sub-string is directly involved in character features and facilitates recognition by exploiting fixed sub-string patterns during short text training. For instance, the next character of sub-string “Cente” is more likely to be “r”. Previously, these fixed patterns were considered as linguistic information. Nevertheless, in long texts, sub-string patterns become intricate, the persistence of fixed sub-string patterns derived from short text training proves to be detrimental to long text recognition. Therefore, the removal of the residual and MLP enhances the recognition of long texts.

Upon setting  $h$  to 2, there is an average improvement of 1.5% in accuracy on LTB compared to other settings. Through the visualization of the attention maps at various  $h$ , as shown in Fig. 8 in the supplementary, it is observed that only two heads exhibit activity when  $h$  exceeds 2. Consequently, when  $h$  is precisely set to 2, each head autonomously contributes to focusing on character positions.

## C Results training on synthetic datasets

The generalization performance of the STR method can be adequately assessed by training on synthetic datasets and evaluating it using real-world benchmarks. Accordingly, we

$h$	Residual	MLP	Common	U14M	LTB	Avg
12	1	1	<b>96.26</b>	85.33	43.33	74.97
	1	0	96.07	84.65	44.54	75.09
8			95.80	84.52	44.74	75.02
			96.02	85.03	45.60	75.55
6			95.81	84.47	45.24	75.17
			95.79	84.40	46.39	75.53
4		0	95.78	84.18	44.08	74.68
		0	95.90	85.00	<b>47.00</b>	<b>75.97</b>
3			95.68	84.58	46.06	75.44
			96.03	84.88	46.58	75.83
2	1	0	96.04	<b>85.41</b>	45.18	75.54
	1	1				

Table 8: The results about  $h$ , residual and MLP in sub-string matching cross attention.

trained SMTR on the synthetic datasets (Gupta, Vedaldi, and Zisserman 2016; Jaderberg et al. 2014) and validated its performance on two short text benchmarks and LTB. The experimental results are presented in Tab. 9 and reveal that when trained on synthetic datasets, SMTR surpasses the previously best method by 0.54% and 5.39% in the two short text benchmark tests, respectively, setting new state-of-the-art records. Moreover, SMTR exhibits outstanding performance on LTB. This unequivocally demonstrates the robust generalization ability of SMTR.

## D Analysis of the visualisations of attention maps

Fig. 7 of the main script displays the recognition results for two long texts and three short texts. Further, the attention map visualizations were conducted for these five samples. Fig. 9 and Fig. 10 exhibit visualizations for the two long texts, while Fig. 11 illustrates the results for the three short texts. These visualizations vividly demonstrate the direct impact of the attention map’s focusing effect on the recognition. As shown in Fig. 9 and Fig. 10, the attention maps of sinAR and PARSeq, when recognizing long texts, exhibit a tendency to skip some characters, resulting in character missing in the recognition results. On the other hand, LISETR’s attention maps show a circular focusing phenomenon, causing repeated character recognition errors by learning incorrect neighborhoods. Furthermore, both LISETR and CTC, assuming horizontal text alignment, face substantial recognition errors on curved or rotated samples, as depicted in Fig. 11. In contrast, SMTR leveraging its character matching mechanism, precisely focuses on character positions and achieves accurate recognition based on the text reading order in both long and challenging short texts. This advantage underscores SMTR’s superior performance over other attention-based methods in addressing OOL challenges and recognizing texts of arbitrary length.

## E Bad cases of SMTR

By analysing the long text prediction results of SMTR, we found its typical error, as illustrated in Fig. 12. SSMTR relies on sub-string matching for recognition. Therefore, when

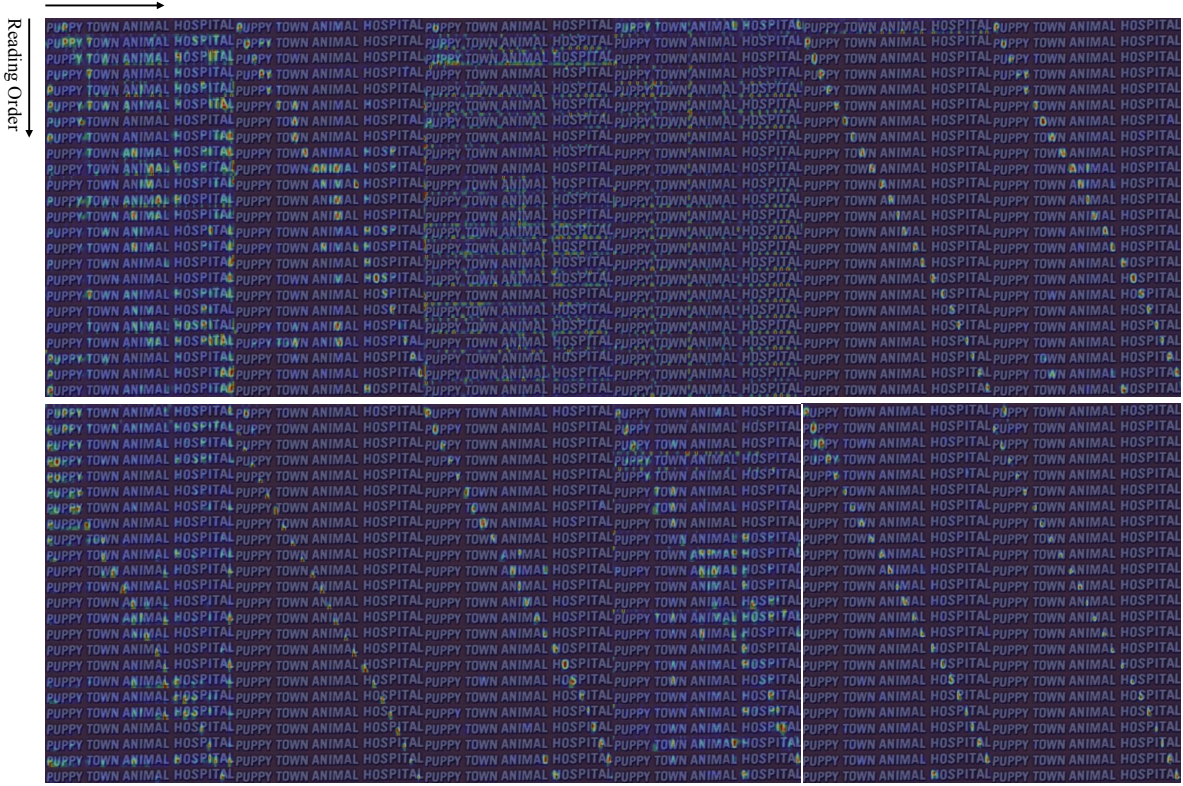


Figure 8: The attention maps  $A_i$  in sub-string matcher when  $h$  is set to 6, 4 and 2.

Method	Common Benchmarks								Union14M-L Benchmarks								LTB	Params ( $\times 10^6$ )
	IC13	SVT	IIIT	IC15	SVTP	CUTE	Avg	CUR	MLO	ART	CTL	SAL	MLW	GEN	Avg			
RoScanner (2020)	94.8	88.1	95.3	77.1	79.5	90.3	87.52	43.6	7.9	41.2	42.6	44.9	46.9	39.5	38.09	0.0	48.0	
SRN (2020)	95.5	91.5	94.8	82.7	85.1	87.8	89.57	63.4	25.3	34.1	28.7	56.5	26.7	46.3	40.14	0.0	54.7	
VisionLAN (2021)	95.7	91.7	95.8	83.7	86.0	88.5	90.23	57.7	14.2	47.8	48.0	64.0	47.9	52.1	47.39	0.0	32.8	
SVTR-B (2022)	97.1	91.5	96.0	85.2	89.9	91.7	91.90	69.8	<b>37.7</b>	47.9	61.4	66.8	44.8	61.0	55.63	0.0	24.6	
PARSeq (2022)	97.0	93.6	97.0	86.5	88.9	92.2	92.53	63.9	16.7	52.5	54.3	68.2	55.9	56.9	52.62	0.0	23.8	
CRNN (2017)	91.1	81.6	82.9	69.4	70.0	65.5	76.75	7.5	0.9	20.7	25.6	13.9	25.6	32.0	18.03	-	8.3	
ASTER (2019)	90.8	90.0	93.3	74.7	80.2	80.9	84.98	34.0	10.2	27.7	33.0	48.2	27.6	39.8	31.50	-	27.2	
NRTR (2019)	95.8	91.5	90.1	79.4	86.6	80.9	87.38	31.7	4.4	36.6	37.3	30.6	54.9	48.0	34.79	-	31.7	
SAR (2019)	91.0	84.5	91.5	69.2	76.4	83.5	82.68	44.3	7.7	42.6	44.2	44.0	51.2	50.5	40.64	-	57.7	
ABINet (2021)	97.4	93.5	96.2	86.0	89.3	89.2	91.93	59.5	12.7	43.3	38.3	62.0	50.8	55.6	46.03	-	36.7	
LPV-B (2023)	97.6	94.6	97.3	87.5	<b>90.9</b>	94.8	93.78	68.3	21.0	<b>59.6</b>	65.1	76.2	63.6	62.0	59.40	-	35.1	
CDisNet (2024)	97.4	93.5	96.4	86.0	88.7	93.4	92.57	69.3	24.4	49.8	55.6	72.8	64.3	58.5	56.38	-	65.5	
LISTER (2023)	<b>97.9</b>	93.8	96.9	87.5	89.6	90.6	92.72	56.5	17.2	52.8	63.5	63.2	59.6	65.4	54.05	24.1	49.9	
SMTR	97.4	<b>94.9</b>	<b>97.4</b>	<b>88.4</b>	89.9	<b>96.2</b>	<b>94.02</b>	<b>74.2</b>	30.6	58.5	<b>67.6</b>	<b>79.6</b>	<b>75.1</b>	<b>67.9</b>	<b>64.79</b>	39.6	15.8	

Table 9: Results on short text benchmarks and LTB tested against existing models when trained on synthetic datasets.

there are two identical sub-strings in a text, SMTR is unable to match the current sub-string correctly, leading to the loop and jump recognition. Notably, this error serve to underscores SMTR's mechanism of employing sub-string matching from the opposite side.

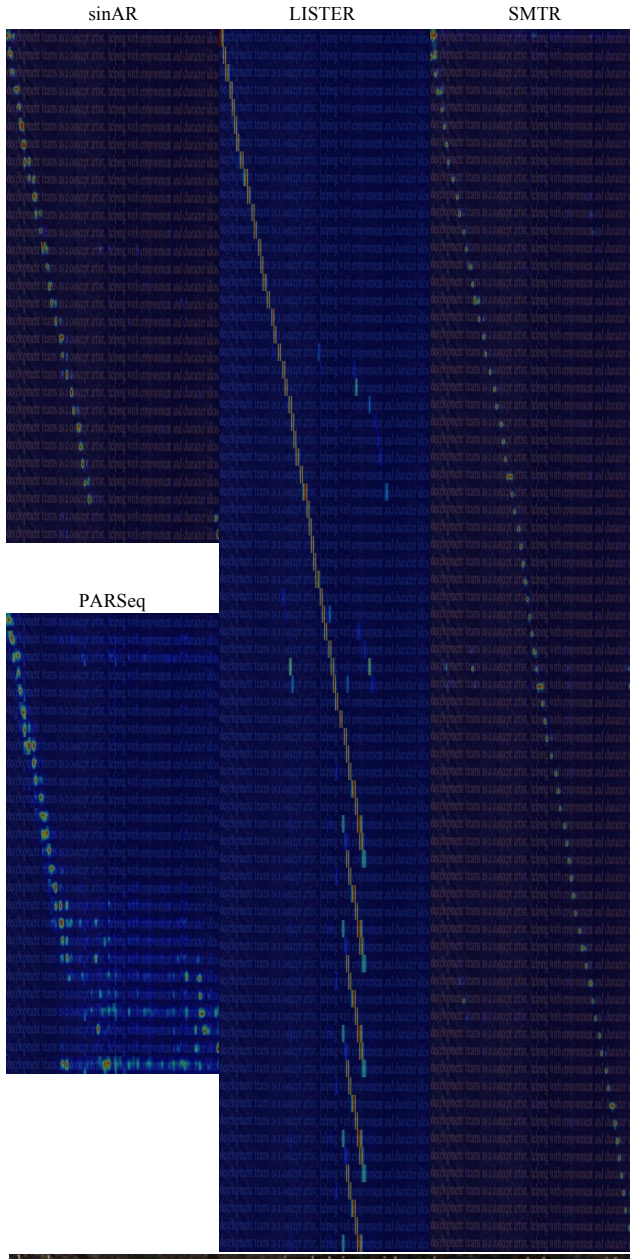


Figure 9: Comparison of the attention map visualisations and prediction results on the first long text.

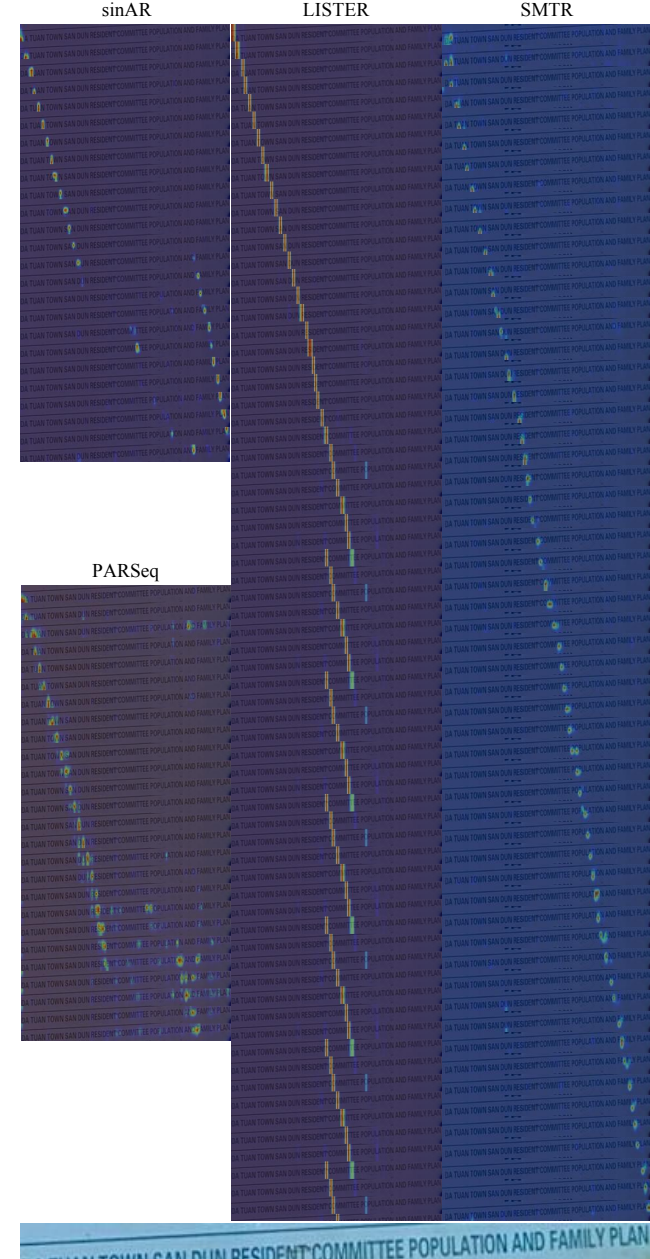
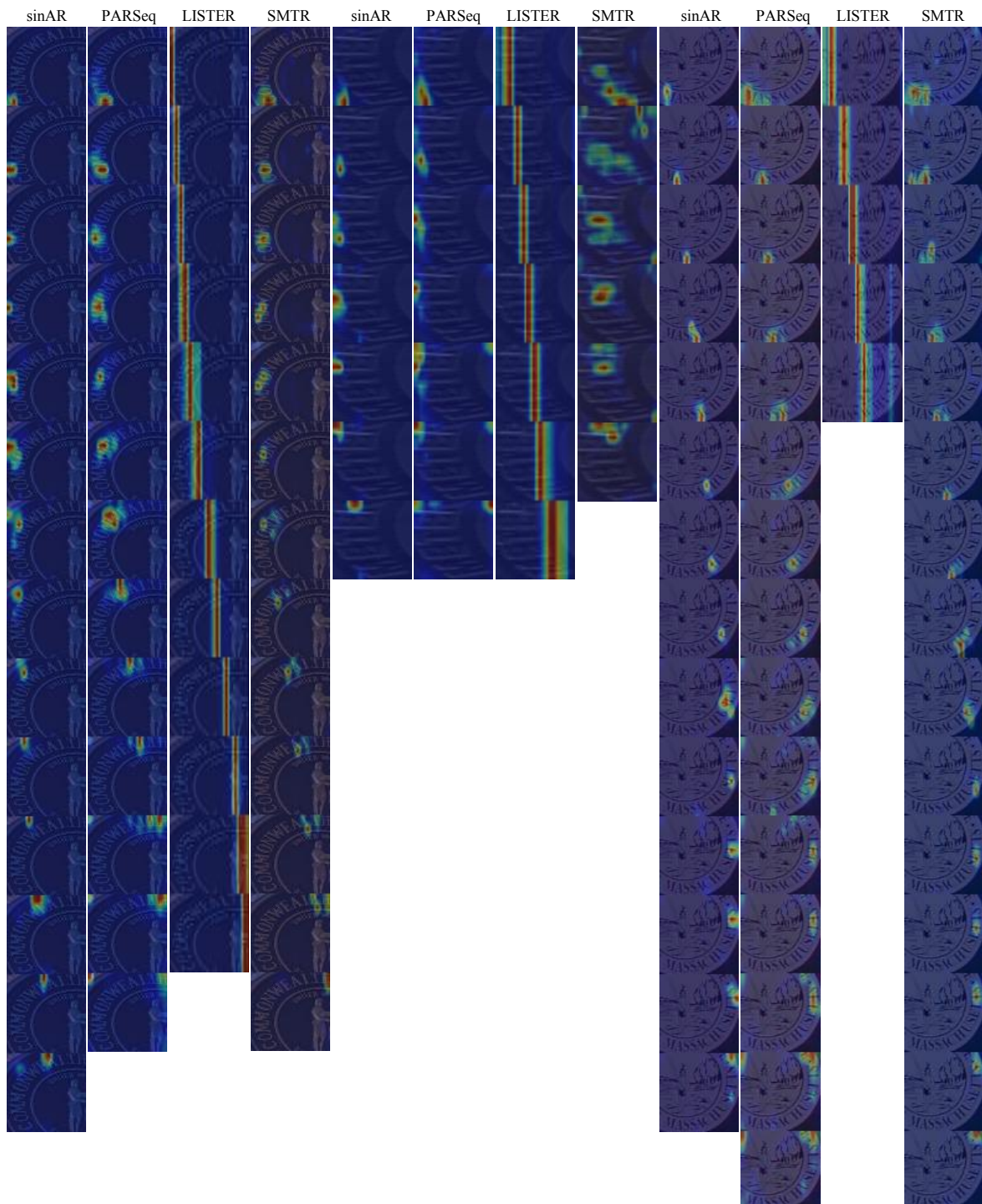


Figure 10: Comparison attention map visualisations and prediction results on the second long text.



CTC: c \_\_\_\_\_ a  
 sinAR: common**is**wealth  
 PARSeq: common**wea**th**th**  
 LISTER: **tereewa** \_\_\_\_\_ alle  
 SMTR: common**wealth**

CTC: se \_\_\_\_\_  
 sinAR: **te**ct**er**  
 PARSeq: **ket**ter  
 LISTER: **ae**et**la**  
 SMTR: meter

CTC: \_\_\_\_\_ a \_\_\_\_\_  
 sinAR: **h**ass**ic**hus**etts**  
 PARSeq: mass**ic**hus**et**ish  
 LISTER: mans \_\_\_\_\_  
 SMTR: mass**ac**hus**etts**.

Figure 11: Comparison of attention map visualisations and prediction results on the three short texts.

I will oppose diverting any Social Security revenues to fund private investment accounts or substituting private investment accounts for Social Security benefits.

Figure 12: Two samples of typical error in SMTR. The presence of identical sub-strings in a text is responsible for both loop and skip recognition.